Elastomeric Nanoparticle Composites Covalently Bound to Al_2O_3/GaAs Surfaces

Hyon Min Song,[†] Peide D. Ye,[‡,§] and Albena Ivanisevic*,[†,||]

Department of Chemistry, Birck Nanotechnology Center, School of Electrical and Computer Engineering, and Weldon School of Biomedical Engineering, Purdue University, West Lafayette, Indiana 47907

Received April 5, 2007. In Final Form: June 14, 2007

This article reports the modification of Al_2O_3/GaAs surfaces with multifunctional soft materials. Siloxane elastomers were covalently bound to dopamine-modified Al_2O_3/GaAs semiconductor surfaces using MPt (M = Fe, Ni) nanoparticles. The sizes of the monodisperse FePt and NiPt nanoparticles were less than 5 nm. The surfaces of the nanoparticles as well as the Al_2O_3/GaAs substrates were modified with allyl-functionalized dopamine that utilized a dihydroxy group as a strong ligand. The immobilization of the elastomers was performed via a hydrosilation reaction of the allyl-functionalized dopamines with the siloxane backbones. X-ray photoelectron spectroscopy (XPS) experiments confirmed the covalent bonding of the siloxane elastomers to the oxide layer on the semiconductor surface. Fourier transform-infrared reflection absorption spectroscopy (FT-IRRAS) measurements revealed that the allyl functional groups are bonded to the siloxane backbones. The FT-IRRAS data also showed that the density of the allyl groups on the surface was lower than that of the siloxane backbones. The mechanical properties of the surface-bound nanocomposites were tested using nanoindentation experiments. The nanoindentation data showed that the soft matrix composed of the elastomeric coating on the surfaces behaves differently from the inner, hard Al_2O_3/GaAs substrate.

Introduction

The "grafting-from" method provides a powerful route to the functionalization of substrates with polymers by using preformed tethered initiators and has been widely used to produce dense, homogeneous molecular layers on surfaces.[1−4] Studies in the literature have shown that one can utilize living radical polymerization,[5−10] plasma polymerization,[11−13] and ring-opening polymerization[14−16] to form self-assembled monolayers of the initiators and avoid local aggregation or condensation. The resulting hydrophobic interface is compatible with a variety of vinyl monomers and can be used to generate covalently bound networks with specific functionalities. Some examples include block copolymer-functionalized silicate,[17] GaAs-PMMA (poly(methyl methacrylate)) hybrids,[18] and chromophore-attached conducting polymers on TiO_2 surfaces.[19] However, relatively few studies have looked at using this methodology to functionalize semiconductor surfaces with polymer/nanoparticle composites. Such composites can increase the utility of the semiconductor surface and can be used to fabricate devices with multiple desirable, tunable properties.

In this report we use the grafting-from polymerization method to prepare multifunctional siloxane elastomers on Al_2O_3-terminated GaAs surfaces. The elastomers were cross linked by dopamine-treated superparamagnetic MPt (M = Fe, Ni) nanoparticles. The motiviation for this work was to immobilize nanoparticles on semiconductor surfaces in a controlled stepwise fashion. Self-assembly methods depending on physical forces can lead to poor film formation and local aggregation of the nanoparticles. Functionalization of the nanoparticle surfaces can enable covalent bonding with different entities. Siloxane−amine conjugation was chosen to make elastomeric siloxane polymers that can act as a stabilizer and prevent the nanoparticles from aggregating. The MPt (M = Fe, Ni) nanoparticles were chosen for their superparamagnetism at room temperature. Polymer/GaAs composites have been widely studied for applications such as flexible inorganic electronics.[20−22] GaAs doped with Al_2O_3 has been used to fabricate metal oxide semiconductor field-

* Author to whom correspondence should be addressed. E-mail: albena@purdue.edu. Tel: 765-496-3676. Fax: 765-496-1459.
[†] Department of Chemistry.
[‡] Birck Nanotechnology Center.
[§] School of Electrical and Computer Engineering.
[||] Weldon School of Biomedical Engineering.

(1) Zhao, B.; Brittain, W. J. *Prog. Polym. Sci.* **2000**, *25*, 677−710.
(2) Stewart, M. P.; Maya, F.; Kosynkin, D. V.; Dirk, S. M.; Stapleton, J. J.; McGuiness, C. L.; Allara, D. L.; Tour, J. M. *J. Am. Chem. Soc.* **2004**, *126*, 370−378.
(3) Wang, Y.; Hu, S.; Brittain, W. J. *Macromolecules* **2006**, *39*, 5675−5678.
(4) Fellah, S.; Ozanam, F.; Chazalviel, J. N.; Vigneron, J.; Etcheberry, A.; Stchakovsky, M. *J. Phys. Chem. B* **2006**, *110*, 1665−1672.
(5) Kim, J. B.; Bruening, M. L.; Baker, G. L. *J. Am. Chem. Soc.* **2000**, *122*, 7616−7617.
(6) Matyjaszewski, K.; Miller, P. J.; Shukla, N.; Immaraporn, B.; Gelman, A.; Luokala, B. B.; Siclovan, T. M.; Kickelbick, G.; Vallant, T.; Hoffmann, H.; Pakula, T. *Macromolecules* **1999**, *32*, 8716−8724.
(7) Ejaz, M.; Yamamoto, S.; Ohno, K.; Tsujii, Y.; Fukuda, T. *Macromolecules* **1998**, *31*, 5934−5936.
(8) Xu, F. J.; Cai, Q. J.; Kang, E. T.; Neoh, K. G. *Langmuir* **2005**, *21*, 3221−3225.
(9) Zhang, M.; Russell, T. P. *Macromolecules* **2006**, *39*, 3531−3539.
(10) Mori, H.; Boker, A.; Krausch, G.; Muller, A. H. E. *Macromolecules* **2001**, *34*, 6871−6882.
(11) Tarducci, C.; Badyal, J. P. S.; Brewer, S. A.; Willis, C. *Chem. Commun.* **2005**, 406−408.
(12) Tarducci, C.; Schofield, W. C. E.; Badyal, J. P. S. *Chem. Mater.* **2002**, *14*, 2541−2545.
(13) Barton, D.; Shard, A. G.; Short, R. D.; Bradley, J. W. *J. Phys. Chem. B* **2005**, *109*, 3207−3211.
(14) Juang, A.; Scherman, O. A.; Grubbs, R. H.; Lewis, N. S. *Langmuir* **2001**, *17*, 1321−1323.
(15) Harada, Y.; Girolami, G. S.; Nuzzo, R. G. *Langmuir* **2003**, *19*, 5104−5114.
(16) Buchmeiser, M. R.; Sinner, F.; Mupa, M.; Wurst, K. *Macromolecules* **2000**, *33*, 32−39.
(17) Zhao, B.; Brittain, W. J. *J. Am. Chem. Soc.* **1999**, *121*, 3557−3558.
(18) Cai, Q. J.; Fu, G. D.; Zhu, F. R.; Kang, E. T.; Noah, K. G. *Angew. Chem., Int. Ed.* **2005**, *44*, 1104−1107.
(19) Senevirathna, M. K. I.; Pitigala, P. K. D. D. P.; Tennakone, K. *J. Phys. Chem. B* **2005**, *109*, 16030−16033.
(20) Tantraporn, W. *Appl. Phys. Lett.* **1979**, *6*, 449−451.
(21) Salata, O. V.; Dobson, P. J.; Hull, P. J.; Hutchison, J. L. *Appl. Phys. Lett.* **1994**, *65*, 189−191.
(22) Manorama, V.; Bhoraskar, S. V.; Rao, V. J.; Kshirsagar, S. T. *Appl. Phys. Lett.* **1989**, *55*, 1641−1643.

10.1021/la700979r CCC: $37.00
Published on Web 07/26/2007

Scheme 1. Stepwise Modification of the Al_2O_3/GaAs Surfaces

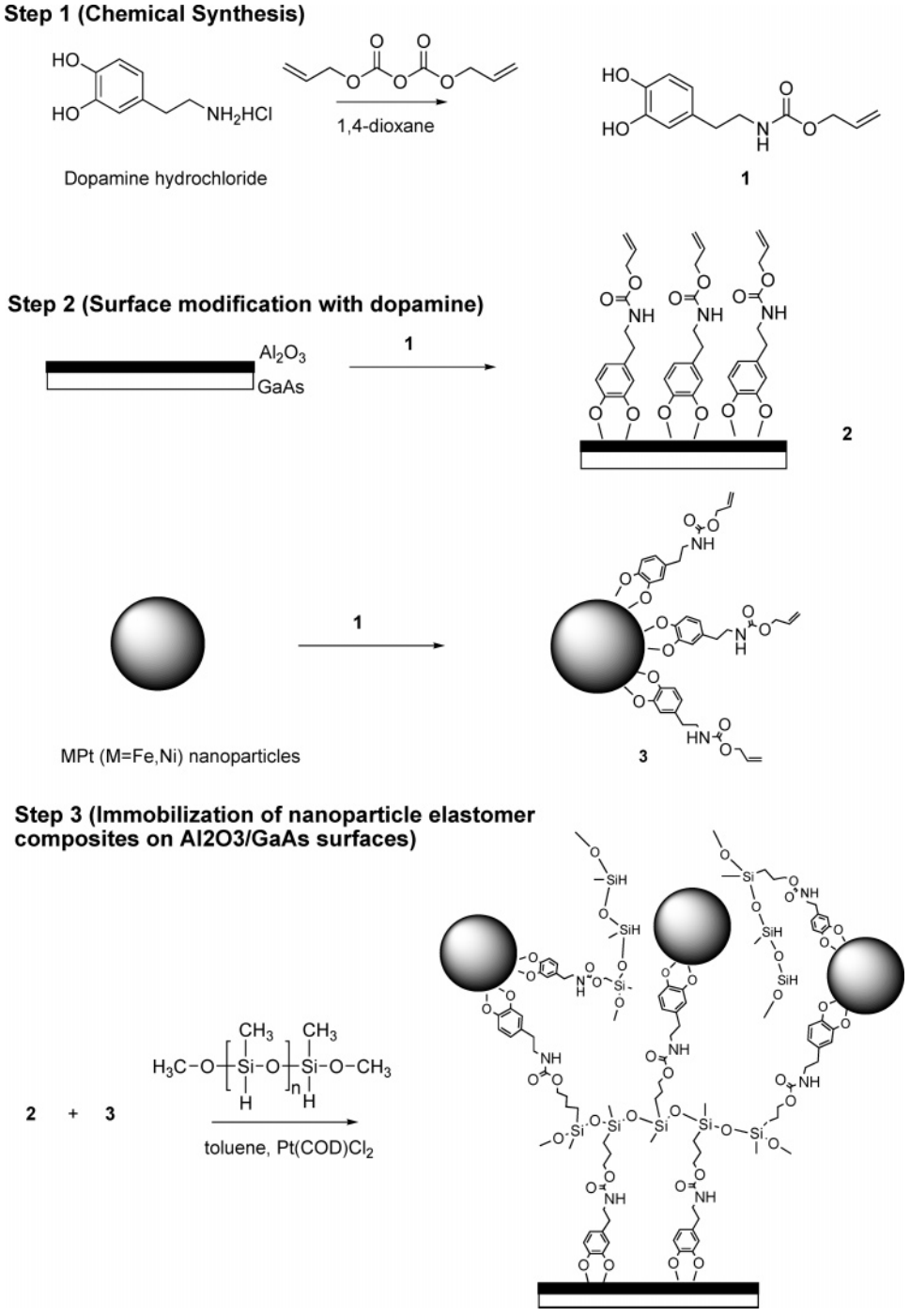

effect transistors (MOSFETs).[23,24] Such devices show great promise because of the intrinsic low noise and high mobility properties of GaAs, and the excellent dielectric insulating properties of Al_2O_3.[25] We chose to explore the functionalization route in Scheme 1 because siloxane polymers on semiconductor surfaces can act as etch masks and lithographic coatings. The incorporation of nanoparticle elastomers on the GaAs surface provides additional characteristics such as magnetic properties and the ability to tune the mechanical properties of the top surface layer.

The main goal of this project is to pattern magnetically active nanoparticles on semiconductor surfaces by a bottom-up approach in order to fabricate dense, homogeneous films on the nanometer scale. Three dimensionally confined magnetic nanoparticles embedded in insulating layers have shown promise for use in nonvolatile flash memory devices,[26] and the results of this report can be utilized in the construction of such devices. The bonding within the composite network is covalent and leads to better

(23) Ye, P. D.; Wilk, G. D.; Yang, B.; Kwo, J.; Chu, S. N. G.; Nakahara, S.; Gossmann, H. J. L.; Mannaerts, J. P.; Hong, M.; Ng, K. K.; Bude, J. *Appl. Phys. Lett.* **2003**, *83*, 180−182.

(24) Ye, P. D.; Wilk, G. D.; Yang, B.; Kwo, J.; Gossmann, H. J. L.; Hong, M.; Ng, K. K.; Bude, J. *Appl. Phys. Lett.* **2004**, *84*, 434−436.

(25) Ye, P. D.; Wilk, G. D.; Tois, E. E.; Wang, J. J. *Appl. Phys. Lett.* **2005**, *87*, 013501-1−013501-3.

(26) Kim, J. H.; Jin, J. Y.; Jung, J. H.; Lee, I.; Kim, T. W.; Lim, S. K.; Yoon, C. S.; Kim, Y. H. *Appl. Phys. Lett.* **2005**, *86*, 032904.

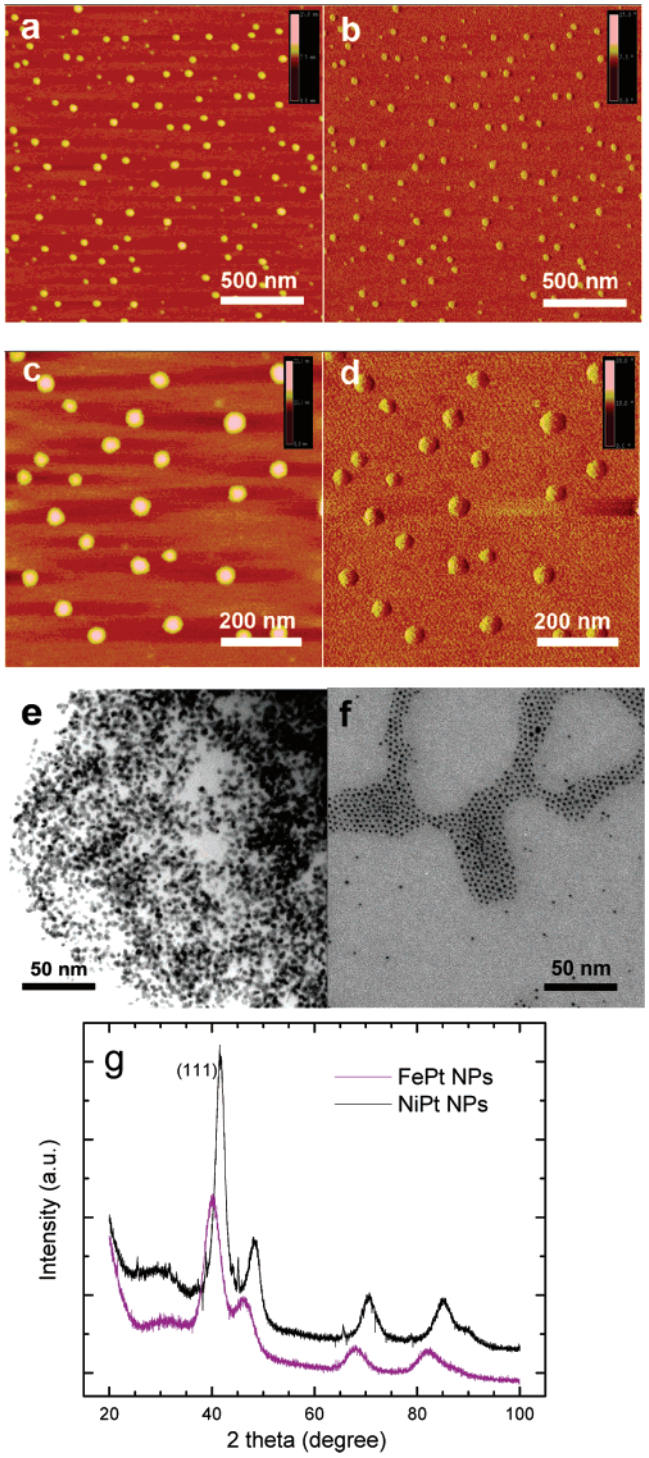

Figure 1. (a) Height AFM image of the as-synthesized NiPt nanoparticles, *z* scale = 15 nm. (b) Phase image of the as-synthesized NiPt nanoparticles, *z* scale = 15°. (c) Height image and (d) phase image of the as-synthesized FePt nanoparticles. The *z* scale is 20 nm for part c and 20° for part d. (e) TEM image of the as-synthesized NiPt nanoparticles and (f) TEM image of the as-synthesized FePt nanoparticles. (g) X-ray powder diffraction patterns of the as-synthesized NiPt (black) and FePt (purple) nanoparticles. Face-centered cubic phases (*Fm*-3*m*) with cell parameters of $a = 3.843$ Å (FePt) and 3.755 Å (NiPt) were identified.

stability compared to that achieved in Langmuir−Blodgett films or in thin films prepared by physisorption. Moreover, in addition to their superparamagnetism, the MPt (M = Fe, Ni) nanoparticles can be used to enforce the overall mechanical properties of the polymer coatings. To the best of our knowledge, this is the first

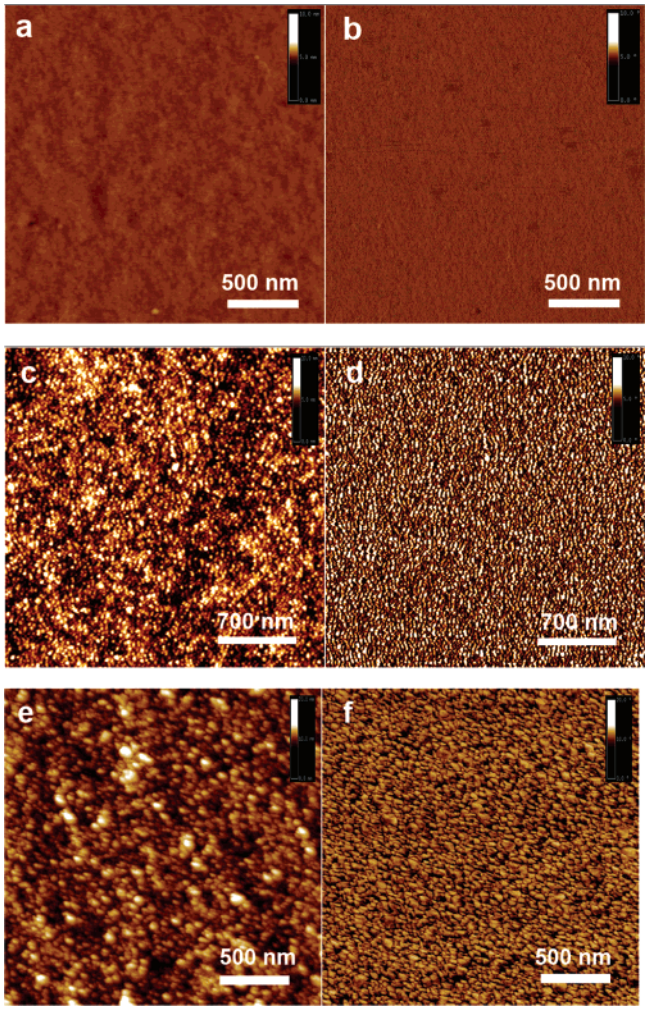

Figure 2. (a) Height and (b) phase AFM images of dopamine-modified Al_2O_3/GaAs surfaces. The *z* scales are 10 nm and 10° in parts a and b, respectively. (c) Height and (d) phase images of the elastomer-immobilized surfaces using NiPt nanoparticles as part of the film. The *z* scales are 10 nm in height and 10° in phase. (e) Height and (f) phase images of the elastomer-bound surfaces using FePt nanoparticles as part of the film. The *z* scales are 20 nm in height and 20° in phase.

report that details the construction of elastomeric FePt and NiPt nanoparticle thin films on this type of surface. Covalent bonding in the composite network is achieved in a chemical way, which is different from traditionally used self-assembly routes.

Experimental Section

General Methods. All chemicals and solvents were used as received without further purification. Air- and water-sensitive reactions employed standard Schlenk techniques under an argon atmosphere. Al_2O_3 (160 Å) on a GaAs substrate was grown via the atomic layer deposition (ALD) method as previously described.[25] Monodisperse FePt and NiPt nanoparticles were prepared using a modified literature procedure where the starting organometallic precursors were $M(acac)_2$ (acac = acetylacetonate) and $PtCl_4$.[27] Powder X-ray diffraction (XRD) of the as-synthesized nanoparticles was measured with a Bruker AXS diffractometer (20 kW) using a graphite monochromator (Cu Kα radiation; $\lambda = 1.54056$ Å). We used the $\theta-2\theta$ scanning method from 20 to 100° (2θ, wide angle). Transmission electron microscopy (TEM) samples were prepared by casting FePt and NiPt nanoparticles in hexane solvent on carbon-

(27) Sun, S.; Anders, S.; Thomson, T.; Baglin, J. E. E.; Toney, M. F.; Hamann, H. F.; Murray, C. B.; Terris, B. D. *J. Phys. Chem. B* **2003**, *107*, 5419−5425.

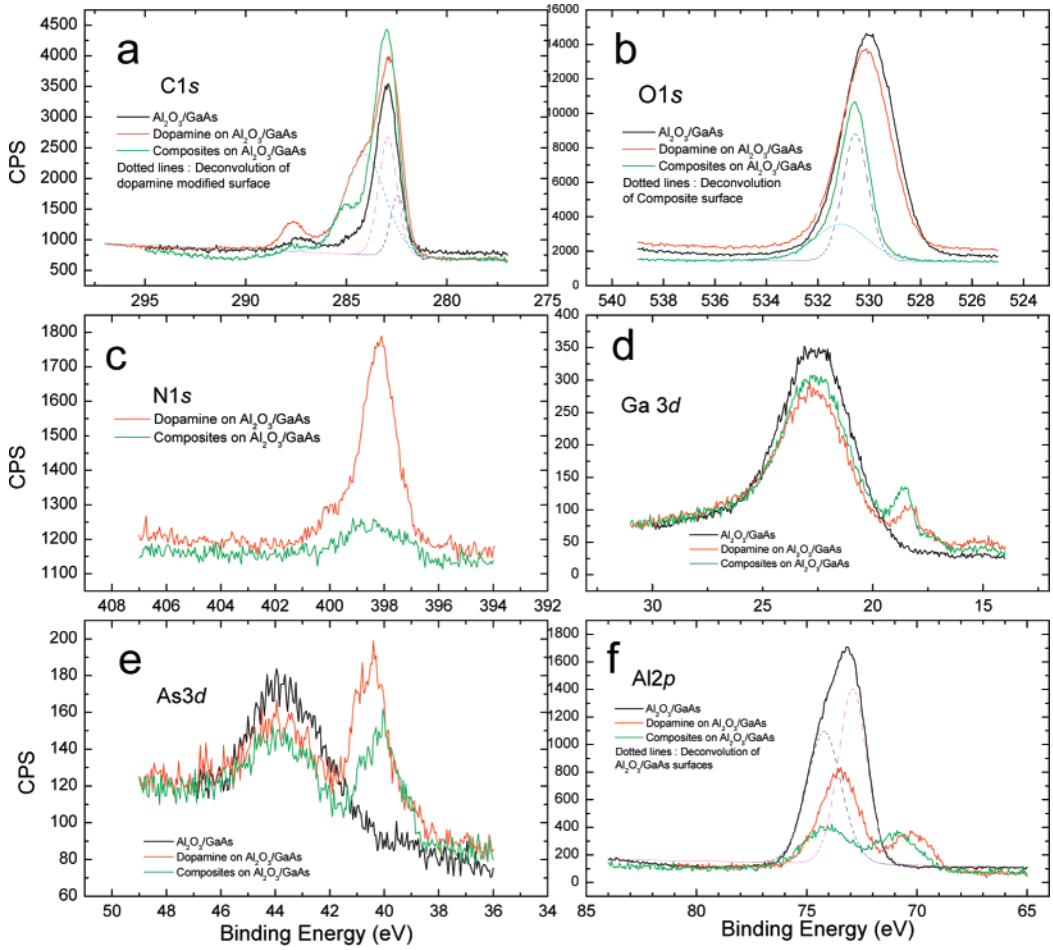

Figure 3. X-ray photoelectron spectroscopy measurement of the Al_2O_3/GaAs substrate (black line), dopamine-treated Al_2O_3/GaAs surface (red line), and surface functionalized with siloxane elastomers (green line). High-resolutions scans of the following regions: (a) C 1s, (b) O 1s, (c) N 1s, (d) Ga 3d, (e) As 3d, and (f) Al 2p.

coated TEM grids. The TEM images were taken with an FEI/Philips CM-100 instrument operated at 100 keV.

Synthesis of *N*-Allyl-3,4-dihydroxyphenylethylamine.[28] Diallycarbonate (5.2 mL, 0.036 mol) was added dropwise for 5 min under an argon atmosphere to stirring reaction mixtures of 1,4-dioxane (50 mL), H_2O (25 mL), dopamine hydrochloride (6.9 g, 0.036 mol), and NaOH (1 M, 25 mL). Stirring was continued for 12 h, and the completion of the reaction was confirmed. Subsequently, the reaction mixture was diluted with 50 mL of ethyl acetate and acidified with dilute HCl solution (1 M) in order to adjust the pH value to 3. The crude mixture was analyzed via chromatography with an eluant of hexane/ethyl acetate/MeOH (3:2:0.5) to give *N*-allyl-3,4-dihydroxyphenylethylamine in 85% yield. ^{1}H NMR (300 MHz, $CDCl_3$): δ 6.75 (m, 2H), 6.56 (m, 1H), 5.90 (m, 1H), 5.25 (m, 2H), 4.97 (s, 1H), 4.55 (m, 2H), 3.36 (t, 2H), 2.73 (t, 2H). ^{13}C NMR (75 MHz, $CDCl_3$): δ 156.07, 145.62, 144.07, 130.81, 119.82, 116.62, 116.10, 78.17, 42.77, 35.85, 29.11.

Surface Modification of Al_2O_3/GaAs with Allyl-Functionalized Dopamine. Small pieces of Al_2O_3/GaAs (0.5×0.5 cm^2) were dipped into a small glass vial containing a mixture of 2 mL of methanol, 5 mL of H_2O, and 30 mg (0.155 mmol) of *N*-ally-3,4-dihydroxyphenylethylamine. HCl (2 drops of a 1 M solution) was added, and the subsequent mixture was sonicated for 30 min. After the aqueous solution was removed, the semiconductor substrate was washed with methanol several times to remove excess unbound dopamine molecules.

Preparation of Surface-Modified FePt and NiPt Nanoparticles. FePt or NiPt nanoparticles (40 mg) were dispersed in 10 mL of hexane solution and mixed with 20 mg (0.103 mmol) of *N*-ally-3,4-dihydroxyphenylethylamine, 5 mL of methanol, and 10 mL of H_2O. The mixture was sonicated for 1 h after the pH value was adjusted to approximately 4. Subsequently, the crude product was centrifuged to remove the aqueous phase. The centrifuging cycle was repeated several times with the addition of methanol. After centrifugation, all solvents were evaporated off under vacuum to leave behind the dopamine-modified FePt or NiPt nanoparticles.

Hydrosilation Reaction of Siloxane Elastomers on Al_2O_3/GaAs. The small vial with the dopamine-treated Al_2O_3/GaAs substrate on the bottom was used, and 3 mL of toluene, 1 mL of hexane dispersed and surface-treated FePt or NiPt nanoparticles (10 mg), and poly(methyl hydrosiloxane) (0.02 mL) were mixed with dichloro(1,5-cyclooctadiene)platinum (1 mg). The vial was placed on a vacuum rotary evaporator with the temperature of the water bath set to 80 °C. The vial was slowly rotated for 20 min under vacuum. The gel-like toluene solution was removed, and the Al_2O_3/GaAs substrate was washed with toluene several times.

Atomic Force Microscopy (AFM) Characterization. AFM images were taken in tapping mode with a silicon nitride tip (model OTESPA7 from Veeco) using a Digital Instruments Nanoscope IIIa. The morphology of the as-synthesized nanoparticles was examined first by dropping nanoparticle-dispersed hexane solution onto mica. Additionally, we characterized the topography and surface roughness of the following samples: (i) GaAs with 160 Å of Al_2O_3, (ii) Al_2O_3/GaAs modified by allyl-functionalized dopamine, and (iii) Al_2O_3/GaAs terminated on siloxane elastomers cross linked by modified FePt or NiPt nanoparticles.

Fourier Transform-Infrared Reflection Absorption Spectroscopy (FT-IRRAS) and X-ray Photoelectron Spectroscopy (XPS) Measurements. FT-IRRAS spectra of the dopamine-modified

(28) Xu, C.; Xu, K.; Gu, H.; Zheng, R.; Liu, H.; Zhang, X.; Guo, Z.; Xu, B. *J. Am. Chem. Soc.* **2004**, *126*, 9938−9939.

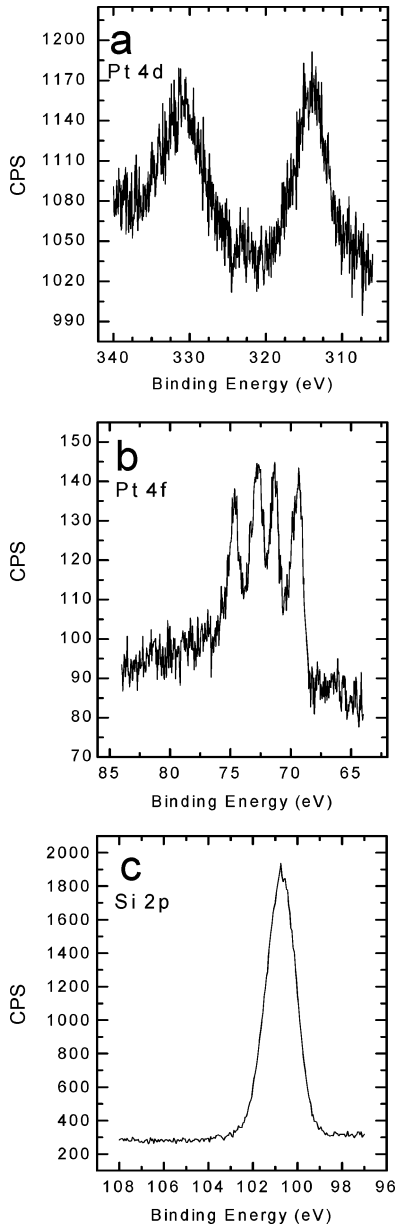

Figure 4. High-resolution XPS scans of the regions corresponding to (a) Pt 4d, (b) Pt 4f, and (c) Si 2p.

Al_2O_3/GaAs substrate and the surface functionalized with siloxane elastomers were collected in single-reflection mode with an FTIR spectrometer (Thermo Nicolet). A Continuum IR microscope was coupled to the instrument, which enabled us to focus the IR beam on the semiconductor surfaces. A narrow-band mercury cadmium−telluride (MCT) detector was used to detect the reflected light. All spectra were collected using 512 scans at a resolution of 2 cm^{-1}. XPS data was collected with an Axis Ultra DLD (Kratos Analytical) instrument equipped with a monochromatic Al Kα X-ray source (1486.7 eV). The pass energy was 160 eV. All XPS spectra were curve fitted with commercially available software (CasaXPS from Casa Software Ltd).

Measurement of Mechanical Properties Using Nanoindentation. Nanoindentation experiments were conducted with a Hysitron Ubi 1 scanning quasistatic Nanomechanical Test Instrument (Minneapolis, MN). The samples tested were (i) GaAs with 160 Å of Al_2O_3, (ii) Al_2O_3/GaAs modified by allyl-functionalized dopamine, and (iii) Al_2O_3/GaAs terminated on siloxane elastomers cross linked by modified FePt or NiPt nanoparticles. Two types of tips were used to measure the mechanical properties: a three-sided pyramidal Berkovich tip (142.3°) and a conical 90° tip. The testing was done in open loop mode with loading and unloading rates of 100 μN/s. Before the indentation measurements on the GaAs surfaces, a tip calibration was performed on a quartz sample with a known reduced elastic modulus (69.6 MPa). The calibration was performed with loading forces between 100 and 7000 μN, and a total of 25 indentations were carried out. The indent area (A) was fitted with the indent depth (h_c) as the variable in the polynomial equation $A = C_0h_c^2 + C_1h_c + C_2h_c^{1/2} + C_3h_c^{1/4} + C_4h_c^{1/8} + C_5h_c^{1/16}$.[29] The C_0 value was set to 24.5 for the Berkovich tip and to 2.598 for the conical 90° tip. The C_1-C_5 terms were fit to the curve. The unloading curves were used to analyze the reduced elastic modulus and hardness of the samples using a power law fitting.

Results and Discussion

In this section, we present our detailed characterization of the modified Al_2O_3/GaAs substrates. We utilized surface-sensitive techniques in order to understand the morphology and composition of the elastomeric composite on the semiconductor surface. The techniques that we chose also allowed us to collect evidence that supports the formation of covalent bonds within the surface-anchored composite network as depicted in Scheme 1. We also report the mechanical properties of the composites and compare the measured hardness and elastic modulus values.

MPt (M = Fe, Ni) Nanoparticle Characterization. Both types of nanoparticles were synthesized on the basis of a literature method where the starting organometallic precursors were $M(acac)_2$ (acac = acetylacetonate) and $PtCl_4$.[27] The as-synthesized particles were initially characterized by AFM after they were cast on mica from hexane dispersions (Figure 1a−d). The z scale in the height images for the NiPt nanoparticles is 15 nm, and the phase images' lag scale is 15° (Figure 1a,b). The FePt nanoparticles are displayed in Figure 1c,d, where the z scale is 20 nm for the height data and 20° for the phase image. The average diameter was determined from TEM images to be 3.2 nm for the NiPt nanoparticles (Figure 1e) and 3.6 nm for the FePt nanoparticles (Figure 1f). We note that others have reported that such size distributions extracted from TEM images can be unreliable because of difficulties (i.e., lack of adequate contrast) associated with counting small particles.[30] From the X-ray diffraction pattern, the face-centered cubic (fcc, *Fm*-3*m*) phases were identified with cell parameters of $a = 3.843$ Å (FePt) and 3.755 Å (NiPt) (Figure 1g).

Surface Modification and Immobilization of the FePt and NiPt Nanoparticles on Al_2O_3/GaAs Surfaces. The siloxane elastomers are used as an interface between the nanoparticles and the surface. A common way of synthesizing nanoparticle polymer composites is the extraction of preformed nanoparticles into the polymer matrix, which can cause aggregation and phase separation of nanoparticles from the polymers. Controlled stepwise functionalization of nanoparticles and the reaction with the polymer backbones significantly reduce nanoparticle aggregation and even prevent it over very large areas, as seen from the AFM data. Surface functionalization was carried out on the basis of Scheme 1. Allyl-functionalized *N*-ally-3,4-dihydroxyphenylethylamine was synthesized at room temperature under an argon atmosphere through a reaction of 3,4-dihydroxyphenylethylamine hydrochloride with diallyl carbonate in dioxane/H_2O solvent (step 1). This modified dopamine was covalently attached to the Al_2O_3/GaAs substrate and also to the surfaces of the FePt or NiPt nanoparticles (step 2). The final hydrosilation reaction was performed in a toluene solvent at 80 °C with a platinum catalyst. This reaction was between the surface-modified nanoparticles and the polymethylhydrosiloxane moieties

(29) *Ubi 1 User's Manual*; Hysitron Inc.: Minneapolis, MN.
(30) Weibel, A.; Bouchet, R.; Boulc'h, F.; Knauch, P. *Chem. Mater.* **2005**, *17*, 2378−2385.

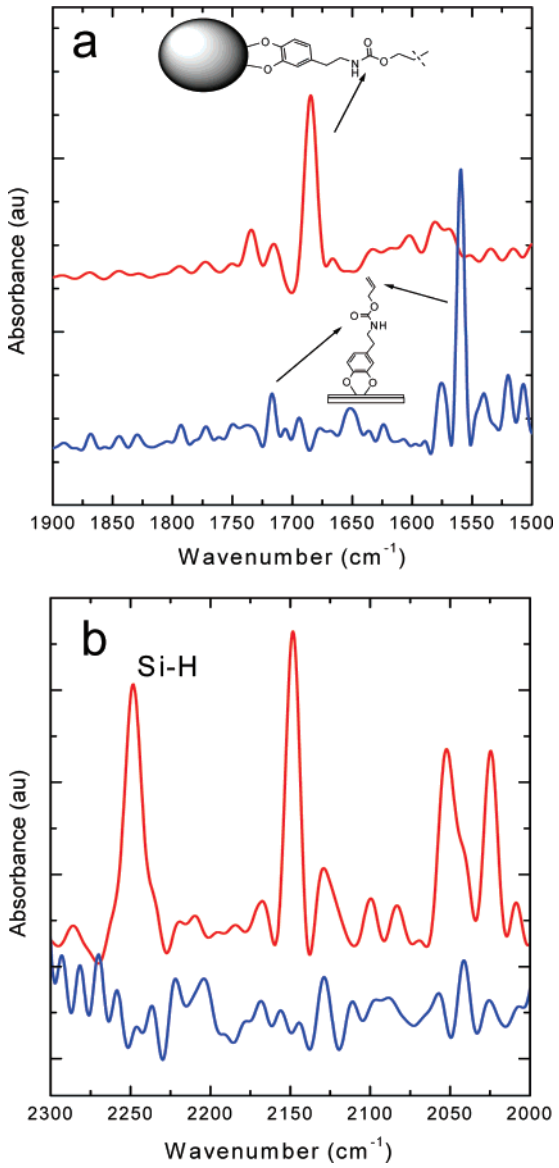

Figure 5. FT-IRMAS absorbance spectra of the dopamine-modified Al_2O_3/GaAs surface (blue) and the elastomer-functionalized Al_2O_3/GaAs surface. (a) The allyl functionality at 1560 cm^{-1} disappears and the amide bonding at 1685 cm^{-1} appears after the hydrosilation reaction. (b) Strong Si−H bonding appears because of unreacted Si−H bonds in the hydrosilation reaction of the allyl functional group with a siloxane backbone.

present on the dopamine-treated semiconductor surfaces (step 3). On the basis of the three-step modification scheme, we expect that the nanoparticles are anchored within the composite via covalent bonds.

The Al_2O_3/GaAs surface morphology was characterized after each modification step, and AFM images are displayed in Figure 2. The topography and phase images of the dopamine-treated Al_2O_3/GaAs substrates (Figure 2a,b) show that the homogeneity of the surface is maintained. The surface morphology changes after the cross-linking step with dopamine-treated NiPt (Figure 2c,d) and FePt nanoparticles (Figure 2e,f). The covalent linkages in the elastomer network can lead to well-dispersed nanoparticles throughout the surface without local aggregation. The AFM data shows very homogeneous and tightly packed particles and indicates that the reaction conditions necessary for the polymerization step do not cause any visible particle aggregation. Some very limited larger clumps can be seen on the AFM images, which we suspect are due to the presence of multilayers on some surface spots. Multilayers can form on the surface, and their formation is dependent upon the density of tethered dopamine on the surface. The thickness of the composite film is projected to be around 6 nm. It is important to note that the thickness of the composite film can be altered by controlling the concentration of the tethered dopamine on the semiconductor surface as well as the coverage of the nanoparticles. The functionalization scheme can, in principle, be used to construct bilayers and multilayers of nanoparticle elastomeric composites.

XPS Measurements. XPS analysis of the Al_2O_3/GaAs substrate, dopamine-treated substrate, and elastomer-immobilized substrate was performed in order to understand the chemical composition of the surface after each functionalization step. Figure 3 displays the high-resolution scans of the major atoms on the Al_2O_3/GaAs surface (black line), the dopamine-modified surface (red line), and the surface functionalized with siloxane elastomers using FePt nanoparticles as part of the composite (green line). Figure 3a is the C 1s region, and it shows significant changes after the dopamine treatment. Upon deconvolution, one can identify a component at 282.4 eV (dotted blue line) due to the aromatic carbons in the dopamine structure, and a peak at 284.2 eV (dotted cyan line) appears as a result of amide bonding in dopamine. This peak shifts to 285.1 eV after siloxane elastomer formation on the Al_2O_3/GaAs surface (green line). The O 1s region (Figure 3b) of the untreated Al_2O_3/GaAs substrate and dopamine-treated surface displays one major peak at 530.1 eV. This species is expected because of the deposition of Al_2O_3 on the GaAs surfaces using ALD. After siloxane elastomer formation, this peak shifts to 530.5 eV. Upon deconvolution of this curve, one finds a component centered at 531.2 eV that is due to siloxane bonding (Si−O−Si). In the N 1s region (Figure 3c), the major peak is centered at 398.1 eV after dopamine treatment of the Al_2O_3/GaAs surface, and it shifts to 398.5 eV upon functionalization with the siloxane elastomer. One also observes a drastic drop in the number of N species on the surface after the polymerization step. No distinct N species were identified on the clean Al_2O_3/GaAs surface.

The XPS data for the Ga 3d and As 3d regions are displayed in Figure 3d,e. Electrons with low binding energies from Ga 3d and As 3d can be emitted in a destructive way when slow scans (high-resolution data) are collected. Electrons from Ga 3d and As 3d can be photoemitted into the upper layer of the material. The core-level binding energies of Ga $3d_{5/2}$ at 22.6 eV and As $3d_{5/2}$ at 43.8 eV correspond to Ga oxides and As oxides, respectively. It is noteworthy that no additional oxide formation was observed after dopamine treatment and the cross linking of siloxane elastomers to the Al_2O_3/GaAs surfaces. We also evaluated changes in the Al 2p high-resolution spectra (Figure 3f). The peak at 74.3 eV corresponds to the oxidized state of Al, and the peak at 72.9 eV corresponds to the metallic state of Al. After dopamine treatment, these two peaks shift to 73.5 and 70.1 eV, respectively, and after elastomer immobilization, they shift to 74.1 and 70.9 eV, respectively.

The XPS analysis identified additional atoms after elastomer modification (Figure 4). An examination of the Pt 4d scan (Figure 4a) reveals the dominant metallic state of Pt 4d with peaks at 313.9 eV ($4d_{5/2}$) and 331.1 eV ($4d_{3/2}$). The small peak centered at 322.5 eV and located between the major peaks stems from the oxidized state of Pt $4d_{5/2}$. An examination of the Pt 4f scan (Figure 4b) shows that there are oxidized Pt species that appear distinctly at 71.3 eV ($4f_{7/2}$) and 74.7 eV ($4f_{5/2}$). These oxidized species are in addition to the metallic Pt that gives rise to peaks at 69.4 eV ($4f_{7/2}$) and 72.8 eV ($4f_{5/2}$). Our XPS analysis showed no evidence of the presence of Fe and Ni on the surface

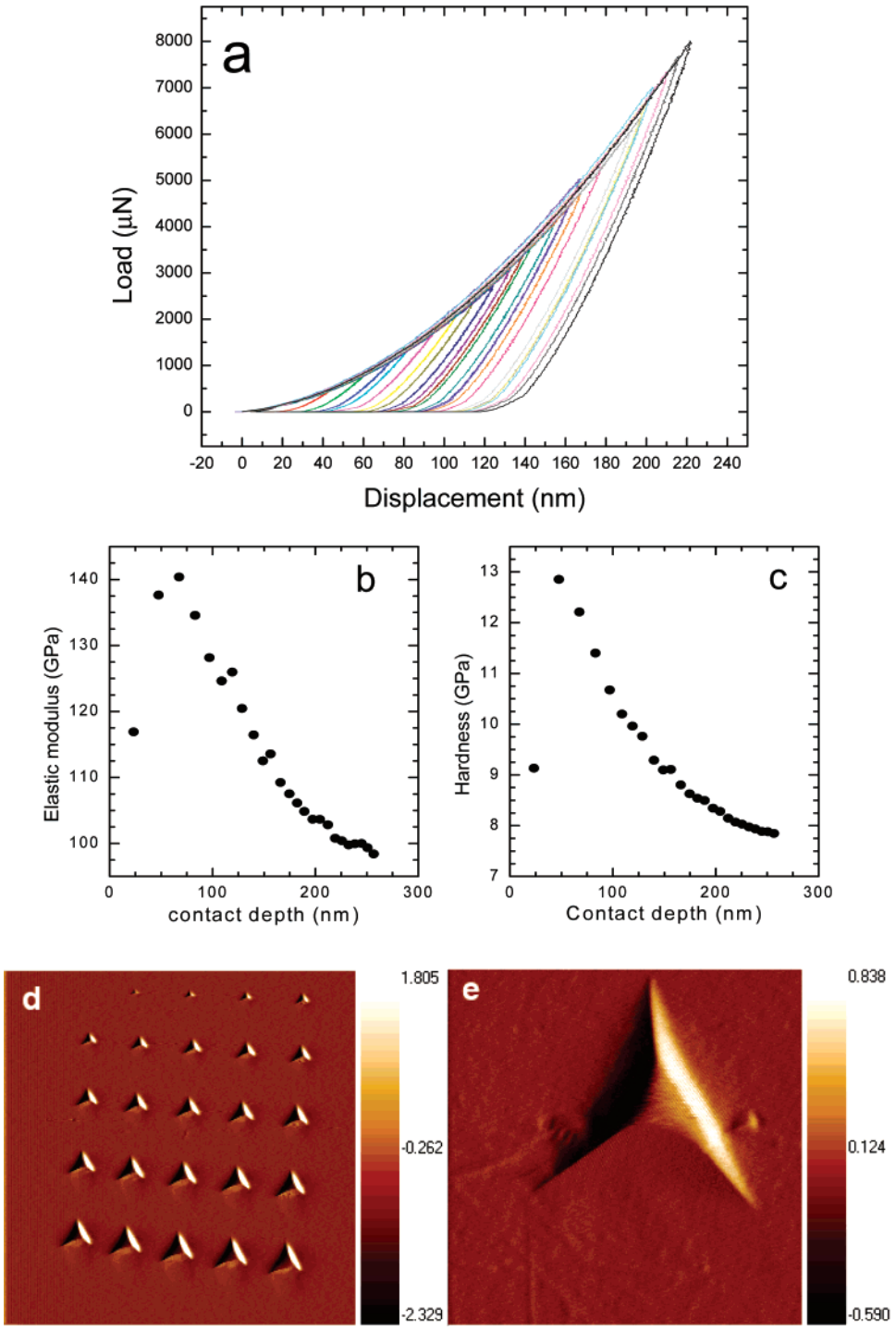

Figure 6. (a) Open-loop nanoindentation profiles of Al_2O_3/GaAs surfaces functionalized with siloxane elastomers. (b) Reduced elastic modulus (E_r) and (c) hardness (H) of the elastomer-coated surfaces vs contact depth. (d) Gradient AFM image of the indentations measured with the sequence in part a. (e) Gradient image of the indentation with an applied load of 2500 μN. The depth bars on the right of the images have units of μN.

after the modified nanoparticles were immobilized in the composite. This observation supports the notion that platinum is the dominant element on the surfaces of the nanoparticles that are imbedded within the siloxane elastomers. On the basis of XPS analysis, Fe and Ni were not found on the elastomer-coated surfaces or on the nanoparticles themselves prior to surface immobilization. The oxidation state of Pt on NiPt before immobilization was observed at 71.3 eV ($4f_{7/2}$) and 74.7 eV ($4f_{5/2}$). This implies that PtO covers the surface of the nanoparticles and prevents other metallic Pt atoms from being oxidized. Fe and Ni are believed to lie in the inner core of the nanoparticles. Our XPS analysis also recorded one major peak at 100.7 eV in the Si 2p scan (Figure 4c) that results from the siloxane backbone of the elastomer.

FT-IRRAS Characterization. The organic functional groups on the dopamine-treated Al_2O_3/GaAs substrate as well as the surface functionalized with siloxane elastomers were studied by FT-IRRAS. The peak corresponding to the alkene (C═C) group at 1560 cm^{-1} (Figure 5a) disappeared after the hydrosilation reaction with the siloxane backbones. After this reaction, a peak centered at 1685 cm^{-1} was observed. This peak is due to the presence of amide bonds on the dopamine-modified surface of

the FePt nanoparticles (red line, Figure 5a). The siloxane linkage also undergoes an absorbance change. Unreacted Si−H bonds appeared at 2250 cm^{-1} after the cross-linking step with the dopamine-modified FePt nanoparticles (red line, Figure 5b). The presence of Si−H bonds implies that the allyl groups on the dopamine-modified Al_2O_3/GaAs surfaces as well as on the surfaces of the FePt nanoparticles underwent a hydrosilation reaction to generate covalently bound elastomer networks on the Al_2O_3/GaAs surfaces.

Nanoindentation Characterization. The mechanical properties of the Al_2O_3/GaAs substrate, dopamine-treated surfaces, and covalently bound surfaces with siloxane elastomers were studied using nanoindentation measurements. The thickness of the elastomer film cannot be measured directly with nanoindentation. The main purpose of conducting the nanoindentation experiment was to find the elastic modulus and hardness of the polymer coating on the solid surfaces. Control of the film thickness depends on the concentration of the tethered dopamine as well as the functionalized nanoparticles and siloxane backbones. Prior to the nanoindentation measurements, the tip was calibrated by making indentations on a test quartz sample. The reduced elastic modulus on the test sample was known. The tip calibration steps are detailed in Supporting Information in accordance with the contact depth and the contact areas of the indentation on the standard quartz sample.

The nanoindentations of the elastomer-coated Al_2O_3/GaAs surface with a maximum load of 8000 μN using an open loop sequence are displayed in Figure 6a. The elastic modulus (E_r, Figure 6b) and hardness (H, Figure 6c) were calculated from the unloading curves. The region near the surface ($E_r = 117.0$ GPa, $H = 9.1$ GPa) has a soft matrix. Until a certain distance is reached, the elastic modulus is at its highest value (140.6 GPa), but then it decreases as the contact depth increases. The hardness also displays similar behavior except that the highest value is at 46 nm, over which the hardness decreases as the indentation contact depth increases.

Indentations with a small load of about 160 μN were applied, and the load displacement was measured (Figure 7). This experiment was done in order to verify the different mechanical properties on the elastomer-coated surface compared to those of the bare Al_2O_3/GaAs surface. When the Berkovich tip was used (Figure 7a), two different matrixes were found. There was a soft matrix of up to 9.8 nm due to the siloxane elasotmers and a hard matrix at over 9.4 nm due to the inner Al_2O_3/GaAs. When the 90° tip was used (Figure 7b), two different mechanical behaviors of the indentations on the elastomer-coated surface were also observed (open symbol). As a reference, indentations on the bare Al_2O_3/GaAs surface were also measured (closed symbol). The indentations on the bare Al_2O_3/GaAs surface showed a homogeneous indentation pattern. With the critical distance of 10.5 nm, the soft elastomeric matrix shows a different loading pattern than does the inner hard Al_2O_3/GaAs matrix. We also prepared MPt (M = Fe, Ni) nanoparticle polymer composites without immobilization on the semiconductor surfaces, as well as elastomers without MPt nanoparticles, in order to compare the mechanical properties of these materials. We evaluated what happens when the nanoparticles were simply imbedded in the elastomers and when these nanoparticle elastomer composites were immobilized on the semiconductor surfaces. Higher tensile strength was observed in FePt nanoparticle composites with elastic modulus ($Er = 1.5$ GPa) and hardness ($H = 0.126$ GPa) values that are greater than for the simple siloxane elastomers ($Er = 0.67$ GPa, $H = 0.115$ GPa). The hardness of the FePt nanoparticle composites was higher than that for the simple siloxane elastomers,

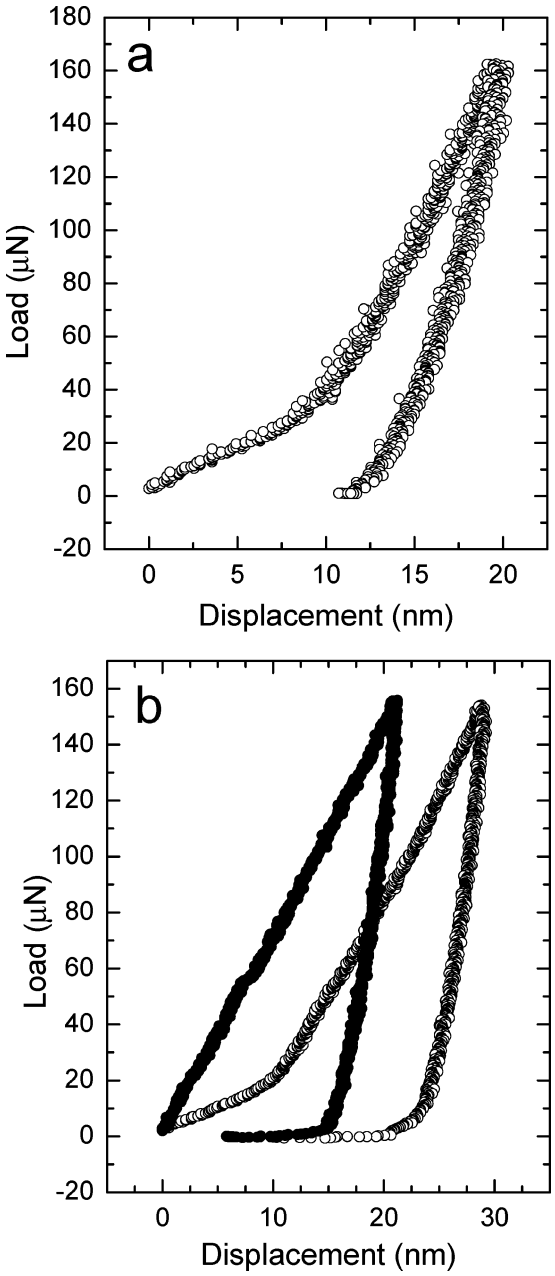

Figure 7. Small-load indentation experiments on the Al_2O_3/GaAs substrate (closed symbols) and the elastomer-coated Al_2O_3/GaAs surface where FePt nanoparticles were used as part of the film (open symbols). (a) Open-loop indentation with a Berkowich tip with a maximum load of 160 μN. (b) Data collected with a 90° tip. The clean Al_2O_3/GaAs substrate without any coating was used as a reference (closed symbols).

which indicates that the composites are more resistant to plastic deformation. Other researchers have also observed that differences in the porosity of structures can contribute to the lowering of indentation hardness.[31] Therefore, our study confirms previous reports that properties extracted from nanoindentation experiments can be correlated with other surface-quality trends. The results in Figure 7 show that the elastic modulus and hardness values ($E_r = 8.1$ GPa, $H = 1.2$ GPa) for the soft matrix of elastomers on the semiconductor surfaces are higher than those for the elastomer composites that were not immobilized on the semiconductor surfaces. The hard matrix in Figure 7 has an elastic modulus and hardness of $E_r = 74.8$ GPa and $H = 6.4$ GPa. In

(31) Kanari, M.; Kawamata, H.; Wakamatsu, T.; Ihara, I. *Appl. Phys. Lett.* **2007**, *90*, 061921.

summary, the indentation experiments in this study were done to find the mechanical properties (elastic modulus and hardness) of the tethered polymers on the semiconductor surfaces. There are many examples of polymer coatings on surfaces, but the mechanical properties of these films have been overlooked. Because a soft elastic matrix on a hard surface can be used as an insulating layer, understanding its properties is important.

Conclusions

We report a method for the immobilization of siloxane elastomers on metal oxide semiconductor surfaces. The method relies on the use of modified magnetic nanoparticles. Our surface-modification scheme enables the preservation of soft elastic properties on the surface. The magnetic FePt and NiPt nanoparticles within the elastomer enable the design and future fabrication of a composite material with tunable magnetic, optical, and catalytic properties. The bonding within the elastomeric network that we create on the surface is covalent, and we recorded little evidence for local aggregation of the nanoparticles on the oxide layer of the semiconductor surfaces. In future studies, the tethering of allyl-functionalized dopamine on the Al_2O_3/GaAs surfaces will be used to pattern elastomer-imbedded nanoparticles in a site-specific manner.

Acknowledgment. This work was supported by NSF under CHE-0614132. We thank Dr. D. Zemlyanov of the Surface Analysis Laboratory at the Birck Nanotechnology Center, Purdue University, for help with XPS analysis.

Supporting Information Available: Additional details regarding the tip calibration procedure used prior to the nanoindentation experiments. This material is available free of charge via the Internet at http://pubs.acs.org.

LA700979R